Manufacturing Letters 36 (2023) 91–95

Contents lists available at ScienceDirect

Manufacturing Letters

journal homepage: www.elsevier.com/locate/mfglet

Letters

Physics-based and data-driven modeling for biomanufacturing 4.0

Michael Ogunsanya, Salil Desai *

Department of Industrial and Systems Engineering, Center of Excellence in Product Design and Advanced Manufacturing, North Carolina Agricultural and Technical State University, Greensboro, NC, USA

ARTICLE INFO

Article history:
Received 2 June 2022
Received in revised form 17 March 2023
Accepted 26 April 2023
Available online 15 May 2023

Keywords:
Biomanufacturing 4.0
Bioprinting
Deep learning
Physics-based model
LSTM

ABSTRACT

Bioprinting involves the fabrication of functional tissue constructs using a combination of biomaterials and it has the potential to transform regenerative medicine. However, bioprinting faces several challenges which can be attributed to its high sensitivity to the slightest variation in process parameters, material constituents, and microenvironmental conditions. This research integrates a physics-based model with a memory-based data-driven model to provide predictive capabilities for bioprinting. The hybrid approach uses the long short-term memory (LSTM) network to provide real-time predictions of the bioprinting process parameters as demonstrated by an illustrated case study.

1. Introduction

Regenerative tissue engineering has been impacted by the emergence of Industry 4.0 which is driven by connectivity, intelligence, and flexible automation [1]. With this, building of scaffolds, printing of tissues and functional organs such as heart [2], lungs, bone [3–5] among others can be accomplished. Currently, bioprinting is patterned around the conventional additive manufacturing processes such as fused deposition modeling (FDM) or stereolithography (SLA) [6]. However, it is sensitive to the slightest variation in material formulations [7–10], process parameters [11–13], microenvironmental conditions [14,15], especially when biologically functional parts are to be printed [16].

Machine learning has been applied in biomanufacturing to unravel hidden, complex, and non-linear patterns that exist in an input–output dataset for applications in computational biology [17], protein synthesis [18], and drug development [19,20] to name a few. Machine learning algorithms [21–24] perform better with big datasets, however big datasets are limited for bioprinting processes due to their high resource intensity [25]. It is worthy to note that, physics-based models alone cannot sufficiently capture the reality that goes into bioprinting as it is based on assumptions made to reduce the model complexity. Thus, it is paramount to incorporate data-driven approaches that can provide comprehensive understanding and predictive capabilities to bioprinting.

Extensive bioprinting experimentation to determine the outcome of a bioprinted part is resource intensive (time and cost). Some works have explored the physics of bioprinting techniques [26,27] however, challenges still exist. These challenges include: (1) just a few reported works provide a framework on bioprinting process, (2) sustaining cell viability [28] and long-term functionality [29], apoptotic effects of bioprinted part based on the sensitive of cells, tissues, process or environmental variation, (3) high cost, long bioprinting time, and resource intensity, and (4) insufficient data repository to aid other forms of data-based prediction models.

For better understanding of the bioprinting process, it is inadequate to use experiments, machine learning, or physics-based model as a stand-alone approach. This research integrates a physics-based model with a memory-based data-driven model to provide predictive capabilities for bioprinting.

2. Methodology

In this research, a hybrid physics-based machine learning model is implemented that integrates the physics-based model by incorporating output of the physics-based model into the long short-term memory (LSTM) network. Fig. 1 shows the framework of the bioprinting process using physics-based data driven model used in this work. A design of experiment was conducted on an extrusion bioprinting process to relate input parameter combinations to the desired bioprinting output. Further, a physics-based model was used to predict bioprinting outcomes for a combination of bioprinting input parameters that could not be obtained from

* Corresponding author.
E-mail address: sdesai@ncat.edu (S. Desai).

https://doi.org/10.1016/j.mfglet.2023.04.003

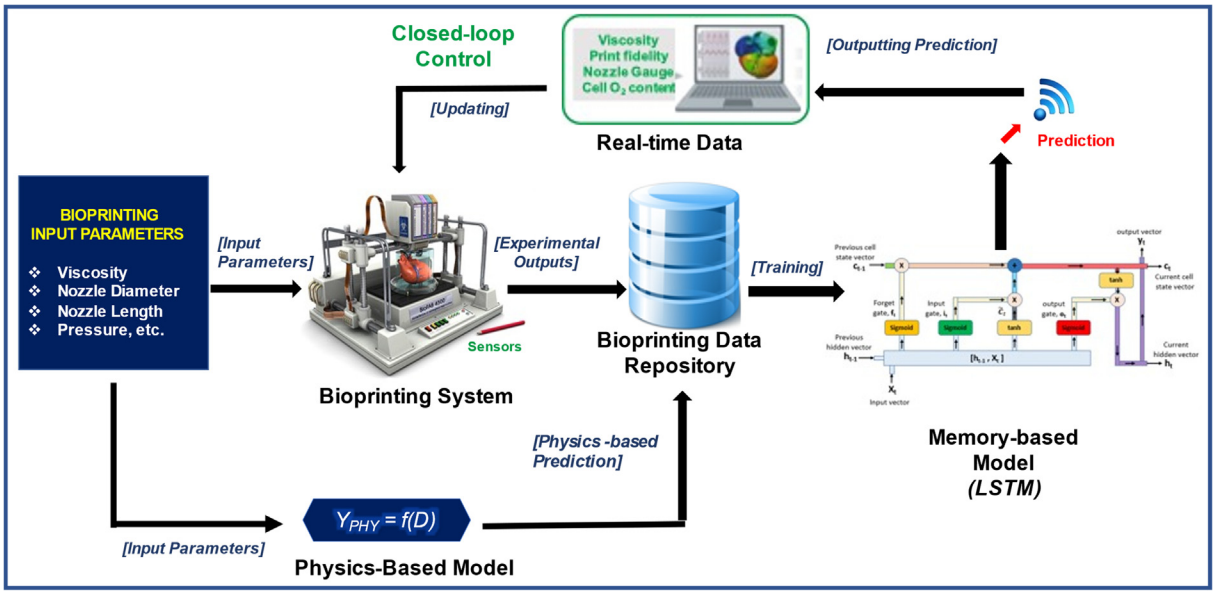

Fig. 1. Physics-based memory-based bioprinting process framework.

experiments. Datasets were obtained using a combination of experiments and physics-based model predictions, thereby, exploring the computational search space for bioprinting. The consolidated datasets were stored in a bioprinting data repository for training the LSTM machine learning model as discussed in detail in Section 2.1. For the next timestamp, the trained LSTM was used to obtain the next output prediction. The prediction and the actual values were compared, and the required update was conducted via closed-loop control. In this section, a formulated hybrid model was used to capture all aspects of bioprinting relating to stem-cell based tissue engineering. These include material formulations, process parameters, and microenvironmental variables. In this bioprinting experiment, a polycaprolactone based matrix (2 to 10 w%/v) was utilized for incorporating calcium magnesium phosphate nanoparticulates [30]. A four-axis Nordson EFD Janome robot with a custom extrusion head was used to fabricate 3D scaffold structures. A sensor array for temperature and humidity (HTU21D-F: GY21) as well as topographical laser mapping (OptoNCDT 1320: Micro Epsilon and Sony IMX322 CMOS) was integrated in the bioprinting process.

2.1. Physics-based model

In this research, an extrusion-based bioprinting process was used as a case-study as shown in Fig. 2. The relation that exists between input parameters (bioprinter specifications, process parameters, and environmental parameters) and desired output was modeled as generalized in **Eq. (1)**.

$$\boldsymbol{Y} = \boldsymbol{f}(\boldsymbol{X}) \tag{1}$$

where, $\boldsymbol{Y}$ is the target output metric (e.g., print resolution, cell viability) and $\boldsymbol{X}$ is the set of input parameters which include material property (e.g., viscosity, density, rheology), process parameter index (e.g., nozzle diameter, speed), and microenvironment index (e.g., temperature, humidity). An extrusion-based bioprinting system uses pressure gradient to deposit bioinks from nozzles using a CAD based tool path layer-by-layer [2]. For the case study, print resolution of printed part was considered as the desired output parameter. Print resolution can be linked to the diameter of strands extruded from the nozzle of the bioprinter. Mathematically, as seen in the works of [26,31], and [25], the resolution of an extrusion-based bioprinting can be modeled by **Eq. (2)**:

$$\boldsymbol{d} = \boldsymbol{D}^2 * \sqrt{\frac{1}{32 * \boldsymbol{\eta} * \boldsymbol{l} * \boldsymbol{v}} * \left(\frac{4\boldsymbol{n}}{3\boldsymbol{n}+1}\right) * \Delta \boldsymbol{P}} \tag{2}$$

The process parameter ranges used in our research are stated. Wherein, $\boldsymbol{d}$ is the resolution of print (20 to 50 μm), $\boldsymbol{D}$ (15 to 50 μm) and $\boldsymbol{l}$ (10 to 40 mm) are diameter and length of nozzle, respectively, $\boldsymbol{v}$ is print speed (2 to 15 mm/s), $\boldsymbol{\eta}$ is apparent viscosity of bioink (50 to 1000 cP), $\boldsymbol{n}$ shear thinning factor (0.5 to 0.9), and $\Delta\boldsymbol{P}$ (20 to 110 kPa) is the gage pressure (pressure drop between the reservoir and nozzle). **Eq. (2)** can be used to generate more print resolution output data for input parameter combinations not considered during experiment.

2.2. Data driven algorithms

After understanding the science of bioprinting and formulating a physics-based model a data-driven approach was implemented to unravel the hidden, complex, and nonlinear relationship that exists between the sets of inputs and outputs. Typically, bioprinting processes build components of tissue scaffolds in a hierarchical fashion [6]. Thus, fabrication of subsequent layers of extra-cellular matrices that are laden with constituent cells and growth factors is highly dependent on prior layers. Moreover, the bioprinting process being highly sensitive to variations in material formulations, process parameters, and microenvironment requires real-time monitoring, prediction, and control at each stage of fabrication. Thus, each layer has a contributing effect to the overall part qualification. This research considers cumulative accuracy and process conditioning for printing of a functional tissue-construct from the initial deposited layer to completion. Memory-based neural networks were used to capture time-transient bioprinting phenomena. Candidate memory models include the recursive neural network (RNN) [32], gated recurrent units (GRU) [33] and long short-term memory network (LSTM) [19]. In the bioprinting process, RNNs are faced with issues of gradient diminishing and explosion problems which are overcome by LSTM. GRU is a special type

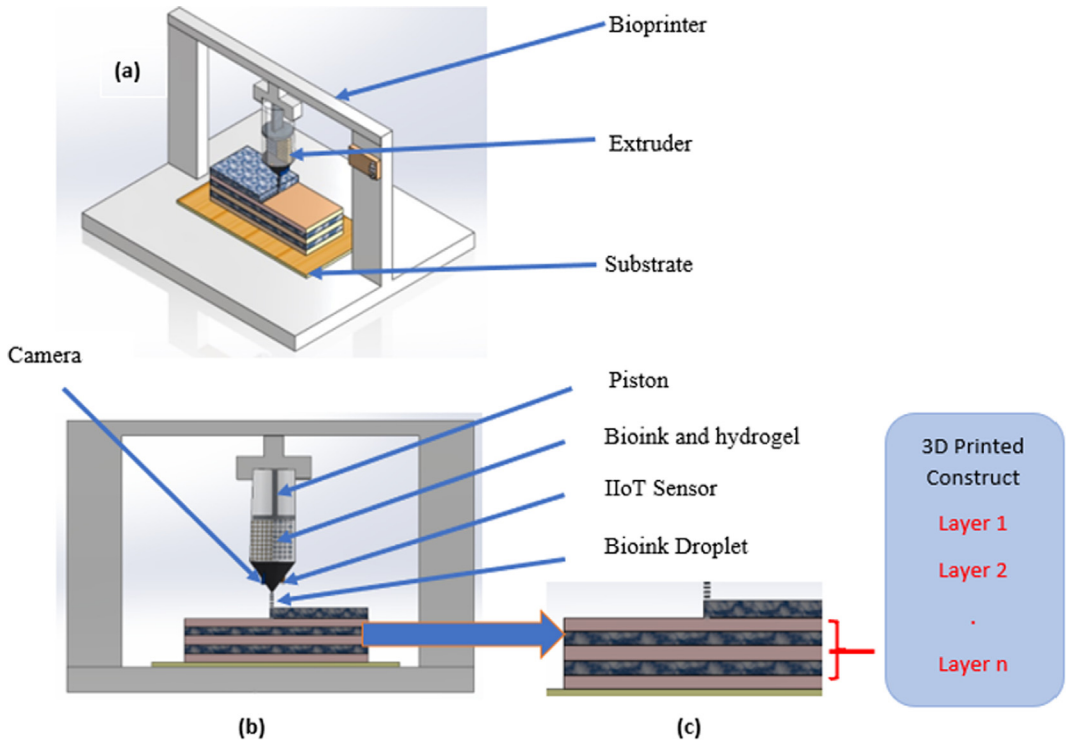

Fig. 2. (a) Isometric view of extrusion-based bioprinter showing set of layered 3D printed construct (b) bioprinter setup with components (c) exploded view of the 3D printed construct and hydrogel on substrate.

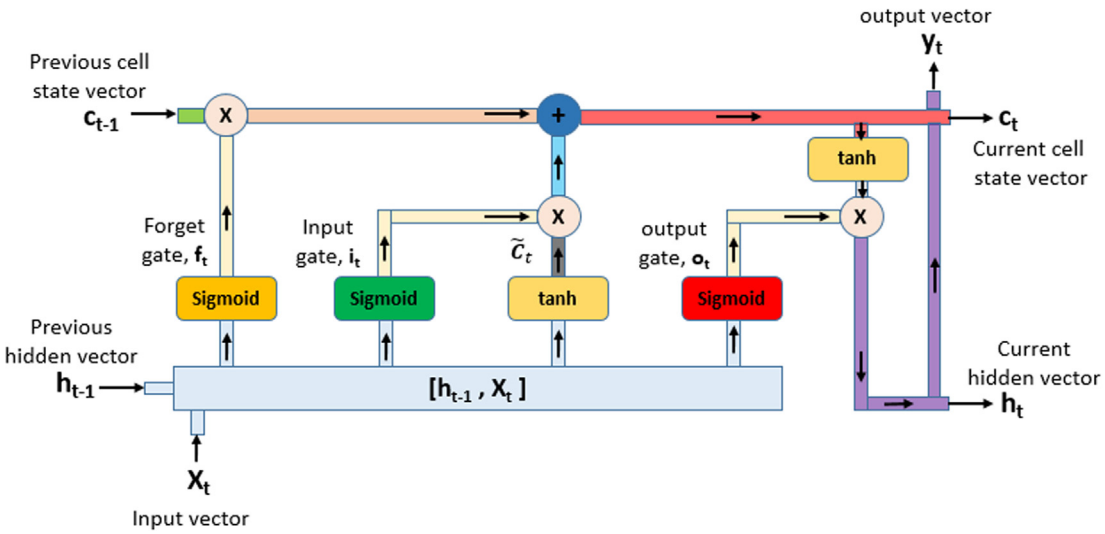

Fig. 3. Simplified and color-coded LSTM Model used for bioprinting.

of LSTM with only two gates. A simplified LSTM network used in this research is shown in Fig. 3.

2.2.1. Incorporating Physics-based model into Machine learning algorithms

For the hybrid model, Eq. (1) was modified to accommodate the output of the physics-based model as given in **Eq. (3)** [34]:

$$\boldsymbol{Y_{HYB}} = \boldsymbol{f_{HYB}}(\boldsymbol{X}, \boldsymbol{Y_{PHY}}) \quad (3)$$

where $\boldsymbol{Y_{HYB}}$ is the prediction from augmenting the original input parameters, $\boldsymbol{X}$, with the output of the physics-based model, $\boldsymbol{Y_{PHY}}$.

2.3. The LSTM regression model

A sequential regressor was instantiated for the LSTM using the TensorFlow module in Python which has an input layer, one hidden layer, and an output layer. From the consolidated dataset, training and test dataset were split according to the considered

time interval. The training and test dataset were further prepared based on our selected timesteps of 3. $(\boldsymbol{X_{training}}, \boldsymbol{Y_{PHY,training}})$ and $\boldsymbol{Y_{HYB,training}}$ were the training data input and output, respectively. Correspondingly we have $(\boldsymbol{X_{test}}, \boldsymbol{Y_{PHY,test}})$ and $\boldsymbol{Y_{HYB,test}}$. Then, a LSTM was instantiated. An input layer was added with units equal to 2, activation function to be ReLU, the return sequence was set to true, and appropriate input shape of (batches, timesteps, features) was maintained as required by LSTM input shape, and a dropout of 0.2 was used. A hidden layer was added with units equal to 5, activation function as ReLU, and a dropout of 0.2. Lastly, an output layer was added with units equal to 1. The LSTM model was compiled with Adam as the optimizer and mean square error (MSE) was used as the loss function. The sequential regressor was fitted on the $(\boldsymbol{X_{training}}, \boldsymbol{Y_{PHY,training}})$ and $\boldsymbol{Y_{HYB,training}}$ with 500 epochs, and a batch size of 1. For the test input data, $(\boldsymbol{X_{test}}, \boldsymbol{Y_{PHY,test}})$, predictions were made on the trained LSTM regressor. Finally, line plots of predicted and actual bioprinted resolutions were obtained to show the capability of the LSTM at different time intervals.

3. Results and discussions

The results of the LSTM model to track and control the bioprinting process based on variations in input conditions are shown in Fig. 4. Five input parameters (viscosity, gauge pressure, growth factor concentration, build orientation, and printing speeds) and $\boldsymbol{Y_{PHY}}$ were considered for an output parameter (print resolution). A combination of these parameters was used to predict two different resolutions for bioprinting - high (20 μm) versus low (50 μm).

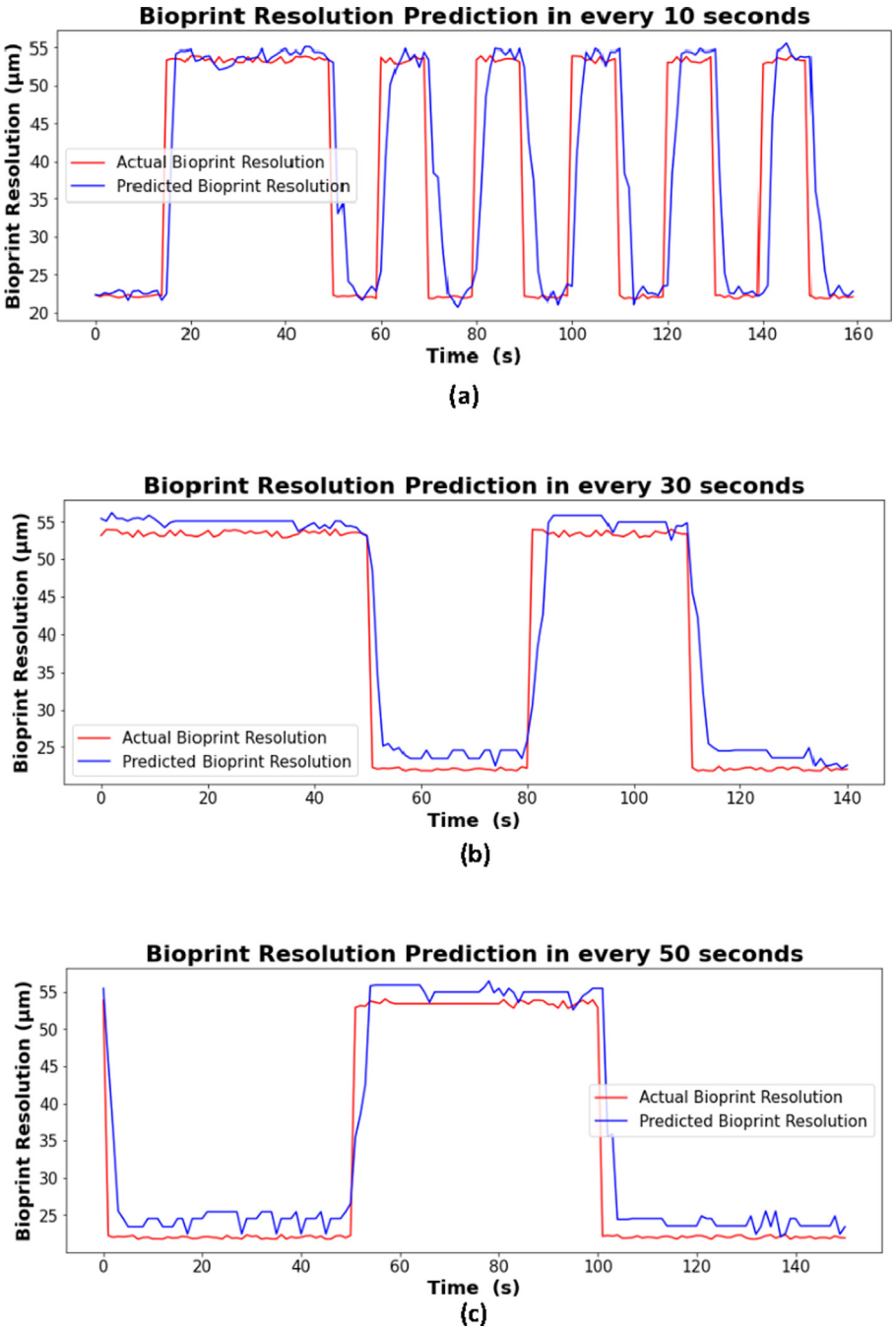

Fig. 4. Bioprinting resolution from IoT sensor against LSTM predictions for (a) 10 s, (b) 30 s, and (c) 50 s feedback.

The LSTM model was tested at different time intervals of 10 s, 30 s, and 50 s, respectively. Fig. 4**a** shows that the LSTM faithfully tracks the actual bioprinted resolution at an interval of 10 s. Fig. 4**b and 4c** shows the resolution at every 30 s and 50 s interval, respectively. However, in these cases there was a slight lag from the LSTM compared to the actual IoT sensor measurements. Although tracking the bioprinting at a short interval (10 s) might seem accurate, capturing data and predicting at higher time intervals (30 and 50 secs) would yield little trade-off in resolution, and save resources. Furthermore, monitoring and capturing data every 10 s could lead to the need for more computer memory and high computational machines. Extended monitoring could serve better if the lag is not large.

From the preliminary results, the LSTM model serves as a means of tracking the events that occur at every layer of the 3D printed construct as seen in Fig. 4. The LSTM network parameters can be tuned based on the type of biomanufacturing process being considered as demonstrated in this research. The optimal input parameters at each layer are further implemented via closed-loop feedback actuators and sensors to effect the necessary change on the next printing layer. Our results shown for bioprinting resolution are extensible to other process parameters, thereby, permitting continuous monitoring and control for optimal tissue regeneration.

4. Conclusions

This paper demonstrates a combination of a physics-based and data-driven model to complement the shortcomings of standalone models in bioprinting process. LSTM was used as the machine learning model based on its ability to track relevant and important information of each layer throughout the process. The impact of different time intervals for updating the LSTM with respect to the desired output was demonstrated. Updating every 10 s shows that the proposed LSTM faithfully tracks the resolution of the bioprinted 3D construct. On the other hand, extended time of 30 s and 50 s show minor lags which could be used for processes where tradeoff are acceptable. Further work should consider including an optimization model which can update the process parameters to enhance the functionality of the bioprinted 3D constructs.

Declaration of Competing Interest

The authors declare that they have no known competing financial interests or personal relationships that could have appeared to influence the work reported in this paper.

Acknowledgment

The authors would like to express their gratitude for funding support from the National Science Foundation Grant (NSF Awards #1663128, #2100739, #2100850, #2200538) and the Center of Excellence in Product Design and Advanced Manufacturing at North Carolina A&T State University.

References

[1] Zhong RY, Xu X, Klotz E, Newman ST. Intelligent manufacturing in the context of industry 4.0: a review. Engineering 2017. https://doi.org/10.1016/J.ENG.2017.05.015.
[2] Zhang YS et al. 3D bioprinting for tissue and organ fabrication. Ann Biomed Eng 2017;45(1):148–63. https://doi.org/10.1007/s10439-016-1612-8.
[3] Adarkwa E, Roy A, Ohodnicki J, Desai S. 3D printing of drug-eluting bioactive multifunctional coatings for orthopedic applications. Int J Bioprinting 2023;110(1).
[4] Adarkwa E, Kotoka R, Desai S. 3D printing of polymeric coatings on AZ31 Mg alloy substrate for corrosion protection of biomedical implants. Med Devices Sensors 2021;4(1). https://doi.org/10.1002/mds3.10167.
[5] Marquetti I, Desai S. Adsorption behavior of bone morphogenetic Protein-2 on a graphite substrate for biomedical applications. Am J Eng Appl Sci 2018;11(2):1037–44. https://doi.org/10.3844/ajeassp.2018.1037.1044.
[6] Cui H, Nowicki M, Fisher JP, Zhang LG. 3D Bioprinting for Organ Regeneration. Adv Healthc Mater 2017. https://doi.org/10.1002/adhm.201601118.
[7] Desai S, Bidanda B, Bártolo PJ. Emerging trends in the applications of metallic and ceramic biomaterials. Bio-Mater Prototyp Appl Med 2021:1–17. https://doi.org/10.1007/978-3-030-35876-1_1.
[8] Desai S, Shankar MR. Emerging trends in polymers, composites, and nano biomaterial applications. Bio-Mater Prototyp Appl Med 2021:19–34. https://doi.org/10.1007/978-3-030-35876-1_2.
[9] Marquetti I, Desai S. Nanoscale topographical effects on the adsorption behavior of bone morphogenetic Protein-2 on graphite. Int J Mol Sci 2022;23(5):pp. https://doi.org/10.3390/ijms23052432.
[10] Bentley J, Desai S, Bastakoti BP. Porous tungsten oxide: recent advances in design, synthesis, and applications. Chem - A Eur J 2021;27(36):9241–52. https://doi.org/10.1002/CHEM.202100649.
[11] Khaled Aldawood F, Andar A, Desai S, Giammona G, Fabiola Craparo E. A comprehensive review of microneedles: types, materials, processes, characterizations and applications. Polym 2021;13(16):2815. https://doi.org/10.3390/POLYM13162815.
[12] Olowe M, Parupelli SK, Desai S. A review of 3D-printing of microneedles. Pharmaceutics 2022;14(12). https://doi.org/10.3390/PHARMACEUTICS14122693.
[13] Desai S, Parupelli S. Additive Manufacturing (3D Printing). In: Maynard's Industrial and Systems Engineering Handbook, Sixth Edition, Springer International Publishing, 2022.
[14] Perkins J, Yi H, Ye SH, Wagner W, Desai S. Direct write manufacturing of controlled release coatings for drug eluting cardiovascular stents. J Biomed Res Part A 2014;102(12):4290–300.
[15] Perkins J et al. Direct writing of polymeric coatings on magnesium alloy for tracheal stent applications. Ann Biomed Eng 2015;43(5):1158–65. https://doi.org/10.1007/S10439-014-1169-3.
[16] Kesti M, Fisch P, Pensalfini M, Mazza E, Zenobi-Wong M. Guidelines for standardization of bioprinting: a systematic study of process parameters and their effect on bioprinted structures. BioNanoMaterials 2016. https://doi.org/10.1515/bnm-2016-0004.
[17] Chicco D, Sadowski P, Baldi P. Deep autoencoder neural networks for gene ontology annotation predictions, 2014, doi: 10.1145/2649387.2649442.
[18] Fa R, Cozzetto D, Wan C, Jones DT. Predicting human protein function with multitask deep neural networks. PLoS One 2018. https://doi.org/10.1371/journal.pone.0198216.
[19] Hochreiter S, Schmidhuber J. Long short-term memory. Neural Comput 1997. https://doi.org/10.1162/neco.1997.9.8.1735.
[20] Arkin A et al. The DOE systems biology knowledgebase (KBase). bioRxiv 2016. https://doi.org/10.1101/096354.
[21] Ogunsanya M, Isichei J, Parupelli SK, Desai S, Cai Y. In-situ droplet monitoring of inkjet 3D printing process using image analysis and machine learning models. Procedia Manuf 2021;53:427–34. https://doi.org/10.1016/j.promfg.2021.06.045.
[22] Elhoone H, Zhang T, Anwar M, Desai S. Cyber-based design for additive manufacturing using artificial neural networks for Industry 4.0. Int J Product Res 2019;58(9):2841–61. https://doi.org/10.1080/00207543.2019.1671627.
[23] Almakayeel N, Desai S, Alghamdi S, Qureshi MRNM. Smart agent system for cyber nano-manufacturing in industry 4.0. Appl Sci 2022;12(12):6143. https://doi.org/10.3390/app12126143.
[24] Akter T, Desai S. Developing a predictive model for nanoimprint lithography using artificial neural networks. Mater Des 2018;160:836–48. https://doi.org/10.1016/j.matdes.2018.10.005.
[25] Ng WL, Chan A, Ong YS, Chua CK. Deep learning for fabrication and maturation of 3D bioprinted tissues and organs. Virtual Phys Prototyping 2020. https://doi.org/10.1080/17452759.2020.1771741.
[26] Suntornnond R, Tan EYS, An J, Chua CK. A mathematical model on the resolution of extrusion bioprinting for the development of new bioinks. Materials (Basel) 2016;9(9). https://doi.org/10.3390/ma9090756.
[27] Paxton N, Smolan W, Böck T, Melchels F, Groll J, Jungst T. Proposal to assess printability of bioinks for extrusion-based bioprinting and evaluation of rheological properties governing bioprintability. Biofabrication 2017. https://doi.org/10.1088/1758-5090/aa8dd8.
[28] Mironov V, Reis N, Derby B. Bioprinting: a beginning. Tissue Eng 2006. https://doi.org/10.1089/ten.2006.12.631.
[29] Tasoglu S, Demirci U. Bioprinting for stem cell research. Trends Biotechnol 2013. https://doi.org/10.1016/j.tibtech.2012.10.005.
[30] Parupelli S, Saudi S, Bhattarai N, Desai S. 3D printing of PCL-ceramic composite scaffolds for bone tissue engineering applications. Int J Bioprint 2023;9(2):0196.
[31] Shafiee A et al. Physics of bioprinting. Appl Phys Rev 2019;6(2). https://doi.org/10.1063/1.5087206. American Institute of Physics Inc..
[32] Caterini AL, Chang DE. Recurrent neural networks. In: Springer Briefs in Computer Science; 2018.
[33] Dey R., Salemt FM. Gate-variants of Gated Recurrent Unit (GRU) neural networks; 2017, doi: 10.1109/MWSCAS.2017.8053243.
[34] Karpatne A, Watkins W, Read J, Kumar V. Physics-guided neural networks (PGNN): an application in lake temperature modeling, arXiv. 2017.